Nano Energy 73 (2020) 104773

Contents lists available at ScienceDirect

Nano Energy

journal homepage: http://www.elsevier.com/locate/nanoen

# Self-powered wearable pressure sensing system for continuous healthcare monitoring enabled by flexible thin-film thermoelectric generator

Yaling Wang [a], Wei Zhu [b,d,*], Yuan Deng [c,d,**], Bo Fu [e,f], Pengcheng Zhu [a], Yuedong Yu [a], Jiao Li [a], Jingjing Guo [g]

[a] School of Materials Science and Engineering, Beihang University, Beijing, 100083, China
[b] Research Institute for Frontier Science, Beihang University, Beijing, 100083, China
[c] Hangzhou Innovation Institute, Beihang University, Hangzhou, 310052, China
[d] Beijing Advanced Innovation Center for Biomedical Engineering, Beihang University, Beijing, 100083, China
[e] BUAA-CCMU Advanced Innovation Center for Big Data-Based Precision Medicine, Interdisciplinary Innovation Institute of Medicine and Engineering, Beihang University, Beijing, 100191, China
[f] School of Instrumentation and Optoelectronic Engineering, Beihang University, Beijing, 100191, China
[g] State Key Laboratory of Precision Measurement Technology and Instruments, Department of Precision Instruments, Tsinghua University, Beijing, 100084, China



ARTICLE INFO

*Keywords:*
Thin-film thermoelectric generator
Thermal-conductivity insulation films
Harvesting body heat
Self-powered pressure sensor
Healthcare monitoring

ABSTRACT

Flexible and portable pressure sensors with highly sensitive and cost-effective attributes are of great demand in wearable electronics, biomedical monitoring, and artificial intelligence. To realize portable pressure sensors with mobile operation, ultrathin, flexible, and sustainable power sources are highly desired. Here, a self-powered wearable pressure sensing system is developed by integrating a conductive elastomer-based pressure sensor with a flexible thin-film thermoelectric generator (tf-TEG) to harvest body heat. Laser engraving technique is adopted to achieve pressure sensor with tunable sensitivity through the controllable design of surface microstructures. To produce a reliable and renewable power supply for the pressure sensor, the flexible tf-TEG is constructed with high thermal-conductivity insulation films for heat absorbing and flexible hydrogels as heat sink, resulting in a large temperature gradient for high power generation. In particular, the pressure sensitivity of the self-powered system is independent of the temperature gradient across the tf-TEG, allowing it to maintain a stable performance under various temperature differences between human skin and surroundings. For the first time, the self-powered pressure sensing system proposed in this work enables continuous monitoring of human physiological signals and body motions entirely powered by the skin-attachable tf-TEG without an electronic boost circuitry.

## 1. Introduction

Wearable electronics have attracted extensive attention over the past decades due to their important applications in artificial intelligence, healthcare monitoring, medical diagnostics and treatments [1–6]. As one of the most important components in wearable electronics, flexible and skin-attachable pressure sensors, devised to transduce external pressure into an electrical change (e.g. triboelectricity, piezoelectricity, capacitance or resistance), have been extensively used to continuously monitor motion activities and physiological signals of human body [7–11]. Among them, triboelectric or piezoelectric devices can sense the body motions to be self-powered sensors, which are beneficial for measuring the dynamic signals. While piezoresistive or capacitance-based pressure sensors could detect the static signal. However, these piezoresistive or capacitance-based sensors driven by batteries require frequent charging and regular replacement, which is inapplicable for long-time unattended monitoring. Although some types of power sources, including solar cells [12,13], piezoelectric and triboelectric generators [14–16], have been proposed as clean energy harvesters to achieve self-powered wearable electronics, the solar energy and vibration-based energy harvesters are restricted by light intensity and body motion, respectively. Thermoelectric generators (TEGs), which could convert continually released body heat into reliable and renewable energy, provide a plausible solution to power most of sensors

* Corresponding author. Research Institute for Frontier Science, Beihang University, Beijing, 100083, China.
** Corresponding author. Hangzhou Innovation Institute, Beihang University, Hangzhou, 310052, China.
*E-mail addresses:* zhu_wei@buaa.edu.cn (W. Zhu), dengyuan@buaa.edu.cn (Y. Deng).

https://doi.org/10.1016/j.nanoen.2020.104773
Received 17 January 2020; Received in revised form 29 March 2020; Accepted 30 March 2020
Available online 8 April 2020

and microelectronic devices [17,18]. However, conventional bulky TEGs, usually made of rigid ceramic plates and thermoelectric legs, are highly stiff and rigid, which are incompatible with the soft and elastic human skins. To address this limitation, intense efforts have been made to enhance the softness and flexibility of wearable TEGs by using flexible printed circuit board and polymers without sacrificing much energy conversion efficiency [19,20]. For example, Cho et al. reported a flexible TEG filled with proprietary polymer materials between the thermoelectric legs and successfully used it to power a wearable electrocardiography [20,21]. Despite the intriguing performances, the flexible TEG required an electronic boost circuitry due to insufficient output voltage, which would lower the output power of the devices and increase the difficulty in wearing. Additionally, thin-film TEG (tf-TEG) integrated with flexible substrate could be a promising strategy to achieve conformal contact with human skin by virtue of its enhanced flexibility and miniaturized size [22–25]. For example, Deng et al. demonstrated a wearable and skin-attachable tf-TEG for human energy harvesting based on $Bi_2Te_3$-type by using magnetron sputtering technique [24]. However, the practical applications of such devices in self-powered wearable sensing are hindered by their low output voltage due to the challenges associated with the design of high thermal-conductivity absorber and heat sink. Besides, heat absorber and heat sink are most commonly made of conductive metals [20,21], which are uncomfortable to wear and restrict body motions due to their rigid nature. Therefore, the developments of flexible and high thermal-conductivity insulating heat absorber and heat sink are crucial for self-powered wearable devices.

Recently, self-powered stretchable sensors based on organic thermoelectric materials have been investigated [26,27]. Bilotti et al. achieved stretchable self-powered sensors based on the thermoelectric response of PEDOT:PSS/Polyurethane blends, but the structure of the flat cross-sections in their stretchable sensor results in a low sensitivity and slow response time [26], which limits their applications in monitoring the subtle physiological signals (e.g. wrist pulse). More recently, constructing specific surface microstructures on the pressure sensors has been proved to be an effective means to improve the sensitivity and response time [28–30]. In 2018, Ren et al. proposed a graphene-based resistive pressure sensor [29], where a random distributed spinosum microstructure is shaped by using abrasive paper as a mold. In 2019, Zhang et al. reported a highly sensitive flexible piezoresistive pressure sensor [30], in which hybrid porous microstructures were designed and fabricated by employing the Epipremnum aureum leaf and sugar as the template. However, it is difficult to adjust and control the geometrical parameters of the microstructures in a molding process. Therefore, an alternative fabrication technology is highly desired to easily tailor the microstructure surface of the pressure sensor. Laser engraving technique could be used to fabricate the pressure senor with tunable sensitivity and detection range due to its excellent controllability in developing well-defined microstructures [31]. Until now, pressure sensor directly powered by a flexible tf-TEG harvesting body heat for continuous healthcare monitoring has not been achieved yet.

Here, we present the design and fabrication of a self-powered wearable pressure sensing system consisting of a micropatterned conductive elastomer-based pressure sensor and a flexible tf-TEG. The tf-TEG based on thin-film $Bi_2Te_3$-type materials was integrated with high thermal-conductivity flexible polydimethylsiloxane/boron nitride (PDMS/BN) composite films and hydrogel heat sink to achieve a high output voltage from harvesting body heat to power the pressure sensor. The sensitivity of the pressure senor could be adjusted through microstructure control using a simple and cost-effective laser engraving technique. A systematic investigation was performed to facilitate the design of the self-powered pressure sensing system with high sensitivity, fast response time, and long-term reliability. As a proof of concept, we demonstrated the broad applications of the self-powered pressure sensor in monitoring various physiological signals and body motions by using the flexible tf-EG to harvest body heat energy.

## 2. Results and discussion

### 2.1. Concept of the self-powered wearable pressure sensing system

The structure and working principle of the self-powered pressure sensing sysytem is depicted schematically in Fig. 1. As shown in Fig. 1a, the flexible tf-TEG serves as a power supply to drive pressure sensor for real-time wrist pulse measurement. Fig. 1b shows the equivalent circuit diagram of the self-powered pressure sensing system, wherein the tf-TEG is mounted on human wrist skin to convert body heat energy into direct current and then powers the resistive pressure sensor. Fig. 1c exhibits the flexible pressure sensor where the microstructured films were placed face-to-face. The flexible tf-TEG is made of 25 pairs of thermoelements electrically connected in series (Fig. 1d). The hot side of the flexible tf-TEG is packaged by flexible and high thermal-conductivity packaging materials (Fig. 1e), while the cold side is connected to a flexible heat sink (Fig. 1f). The output voltage ($V_o$) of the TEG [32,33], the load voltage ($V_L$), and the sensitivity ($S$) of the self-powered pressure sensor are demonstrated by equations (1)–(3), respectively.

$$V_o = n(\alpha_P - \alpha_N)(T_H - T_C) \tag{1}$$

$$V_L = \frac{V_O}{r + R_L} \times R_L \tag{2}$$

$$S = \frac{\partial\left(\frac{V_{L0} - V_L}{V_{L0}}\right)}{\partial P} \tag{3}$$

Where $n$ is the number of the thermocouples, $\alpha_p$ and $\alpha_N$ are the Seebeck coefficients of $p$-$Sb_2Te_3$ and $n$-$Bi_2Te_3$, $T_H$ and $T_C$ are the hot and cold temperatures of the tf-TEG, $r$ is the internal resistance of the tf-TEG, $R_L$ is the load resistance of the sensor, $V_{L0}$ and $V_L$ are the initial load voltage and load voltage under applied pressure ($P$), respectively. If the self-powered pressure sensing system operates successfully, the current of the system must be higher than the working current of the pressure sensor. When the pressure sensor is subjected to external pressure, the change of the load resistance would result in the load-voltage change in the self-powered system.

### 2.2. The design and performance of the flexible tf-TEG for human energy harvesting

In order to obtain high output voltage of the flexible tf-TEG at a small temperature difference, optimizing thermoelectric performance of the $n$-$Bi_2Te_3$ and $p$-$Sb_2Te_3$ can be an effective way according to equation (1). The Te element, due to its volatility, easily reduces at a high sputtering temperature, producing a negative impact on the thermoelectric property of the materials ($n$-$Bi_2Te_3$ and $p$-$Sb_2Te_3$) [34]. Thus, the controllable compensation power of Te in the fabrication process would enhance the thermoelectric performance of $n$-$Bi_2Te_3$ and $p$-$Sb_2Te_3$. Optimizing details of the materials are described in Figs. S1–S4 and the highest thermoelectric properties of the materials at the room temperature are listed in Table 1. It could be observed that the Seebeck-coefficient variation of the optimized thin-film thermoelectric materials could be controlled within a small range ($n$-$Bi_2Te_3$: 130.38–134.57 μV $K^{-1}$, $p$-$Sb_2Te_3$: 133.05–136.75 μV $K^{-1}$) and thus exhibits relatively stable performance in 303–363 K.

With optimized sputtering condition (Table S1), tf-TEG with 25 pairs of thermocouples was fabricated (Figs. S5–S6). The output characteristics of the magnetron-sputtering tf-TEG were first investigated as shown in Fig. 2. The voltage-current and power-current curves were obtained when the temperature difference was varied from 2.3 to 20 K (Fig. 2a and Table S2). With a temperature gradient ($\Delta T$) of 20 K, the tf-TEG produced an output voltage as large as 78 mV and a maximum power of 7.9 μW. The output voltage is linear with respect to $\Delta T$ and the maximum power changes quadratically with the increasing $\Delta T$ (Fig. 2b).

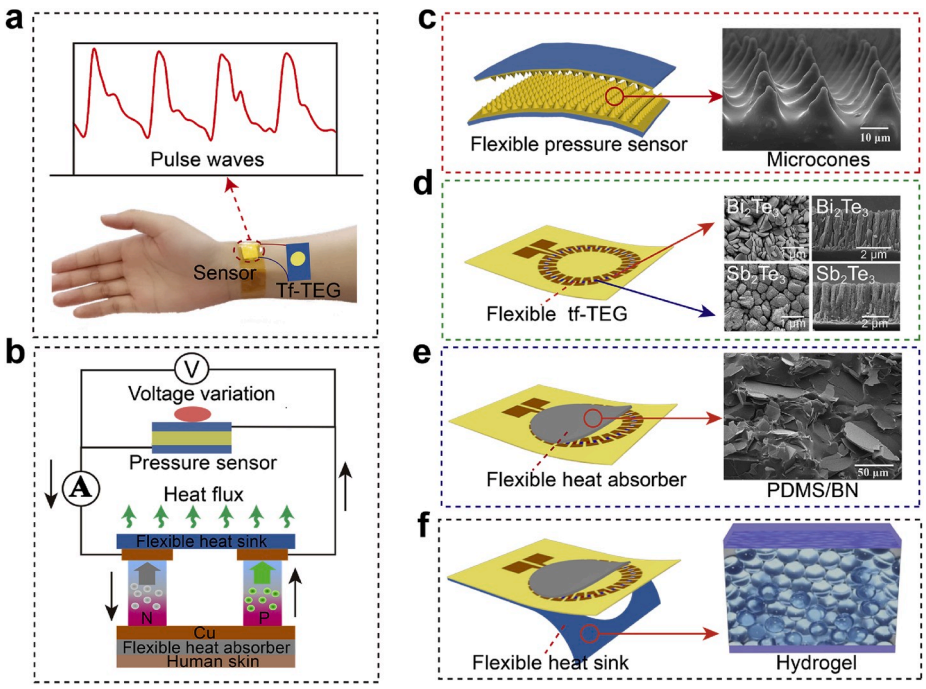


**Fig. 1.** Schematic descriptions and morphology of the self-powered wearable pressure sensing system integrating tf-TEG with a flexible pressure sensor. (a) Schematic illustration of wrist with tf-TEG and pressure sensor equipped. (b) Equivalent circuit diagram of the sensing system. Schematic illustrations of individual components: (c) flexible pressure sensor, (d) flexible tf-TEG, (e) flexible heat absorber, and (f) flexible heat sink.

**Table 1**
Thermoelectric properties of the thin-film thermoelectric materials at room temperature.

| Material type | Electrical conductivity ($\sigma$) [$10^4$ S m$^{-1}$] | Seebeck coefficient ($\alpha$) [$\mu$V K$^{-1}$] | Power factor [$\mu$W cm$^{-1}$ K$^{-2}$] |
|---|---|---|---|
| *n*-$Bi_2Te_3$ | 5.12 | 130.38 | 8.71 |
| *p*-$Sb_2Te_3$ | 10.49 | 133.05 | 18.58 |

FEA was further implemented to verify the open voltage of the thermoelectric device when the hot side of the device was loaded with different temperature (Fig. 2c,d). The open voltage increases with the increasing $\Delta T$ and reaches 79 mV at a $\Delta T$ of 20 K which corresponds with the experimental results in Fig. 2b.

When the tf-TEG is directly attached to human skin, a large thermal resistance from the skin and environment would produce a small temperature difference across the TEG, leading to a low output voltage according to equation (1). In order to reduce the thermal resistance of the

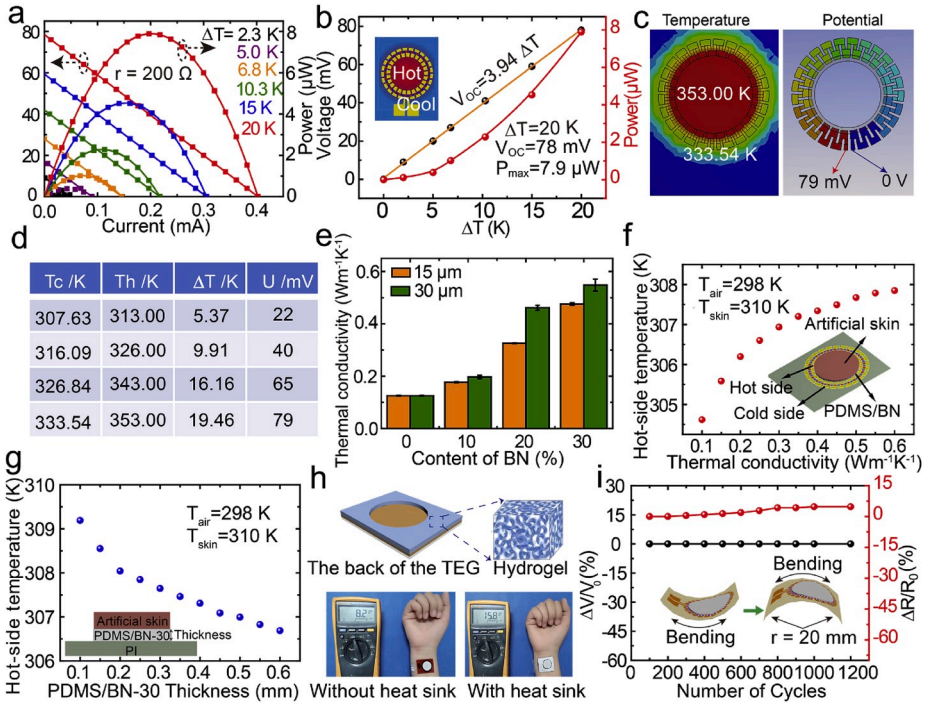


**Fig. 2.** Output performances of the flexible tf-TEG. (a) Voltage-current and power-current curves with respect to $\triangle T$. (b) Output voltage and maximum power at different temperature differences. (c) Temperature and voltage distribution of the tf-TEG at the temperature difference of 19.46 K, obtained by FEA. (d) Simulated open voltage of the TE device generated at different temperature gradients. (e) The thermal conductivity of the PDMS/BN-x composite films. (f) Simulated temperature at the hot side of the tf-TEG versus thermal conductivity of the composite films. (g) Simulated hot-side temperature of the tf-TEG versus thickness of the composite films. (h) A design of the cold side of the tf-TEG (top), and demonstrations of the tf-TEG with/without hydrogel heat sink when it was attached to human skin at ambient temperature of 26 °C (bottom). The PDMS/BN-30 was packaged at the hot side of the tf-TEG. (i) Relative open-circuit voltage($\Delta V/V_0$)and internal resistance ($\Delta R/R_0$) of the tf-TEG under 1200 bending cycles(bending radius r = 20 mm). The inset shows the photograph of the wearable tf-TEG at bending radius of 20 mm.

interfaces, we prepared a thermal conductive packaging material by using elastic PDMS incorporating electrically insulated BN fillers, which are of high thermal conductivity and low electrical conductivity. Fig. 2e shows the thermal conductivity of the composite films under various content of BN. It was found that the thermal conductivity of the composite films gradually increased with the increasing weight of BN fillers. The reason is that the continuous thermal conductive pathway of the composite films was generated gradually by the contact of many BN particles, resulting in the increase of thermal conductivity (Figs. S7–S8). Moreover, it can be also clearly observed that the larger sized BN (30 μm) brings about higher thermal conductivity. It is because that the larger sized BN does not easily agglomerate and could form a smaller contact surface with matrix [35], leading to a smaller total interfacial thermal resistance compared with the smaller sized filler (15 μm) (Figs. S7–S8).

To further elucidate the effect of the PDMS/BN materials on TEG, FEA was conducted to simulate the temperature change of the hot side of the TEG with PDMS/BN when the device was attached to human skin (Fig. 2f). The temperature of the hot side increases with the increasing thermal conductivity of the PDMS/BN due to the reduction of the total thermal resistance, which improves the temperature differences between the flexible TEG and the surroundings (Fig. S9). Besides, composite films with thinner thickness could more easily reduce the thermal resistance from skin and establish a higher temperature gradient across the flexible tf-TEG (Fig. 2g, Fig. S10). However, a simultaneous increase in thermal conductivity and decrease in thickness of the composite films would raise the temperature at the cold side of the tf-TEG (Figs. S9–S10). Thus, a flexible heat sink was necessary in need for temperature cooling at the cold side of the tf-TEG. Hydrogels are three-dimensional network structure containing water. The lager water content of hydrogels enables them to effectively dissipate heat through water evaporation [36], making them an attractive material for heal sinks. Flexible hydrogel heat sink was integrated at the cold side of the TEG and the resulting device showed a remarkable enhancement in the open voltage up to 92% (Fig. 2h). The achieved voltage of flexible tf-TEG is 15.8 mV, which is higher than that of the previously reported skin-attached TEG [19,22,24,32]. Fig. S11 exhibits the voltage output measurement of the wearable tf-TEG with hydrogel heat sink during 8 h. It is observed that the output voltage of tf-TEG is basically stable and maintains a high output level (15.88–14.92 mV).

For long-term healthcare monitoring, the flexible and skin-attached tf-TEG may undergo mechanical deformations during body motion. In Fig. 2i, we investigated the mechanical stability of the device under a bending test, where the tf-TEG was subjected to outward bending at a bending radius of 20 mm. Benefiting from the excellent adhesion between PI and TE materials, the relative changes of the open voltage generated from body heat energy and internal resistance of the tf-TEG were below <5% even after 1200 bending cycles, demonstrating high reliability and stability [24].

### 2.3. Externally powered pressure sensing

Highly sensitive and self-powered pressure sensor is desirable for monitoring physiological signals of human body. Laser engraving technique was adopted to achieve pressure sensor with tunable sensitivity through the controllable design of surface microstructures (Fig. S12). The working mechanism and equivalent circuit of the pressure sensor is demonstrated in Fig. S13, revealing regular coned microstructures of the same feature size. When the pressure sensor was subjected to an external force, the coned patterns would be deformed, leading to an increase of the contact area between the two opposite microconed surface. As a result, there would be a decrease in both the resistance and the load-voltage of the sensor. When the pressure was released, the cones would recover to their base status due to the elastic performance of PDMS [37]. To obtain a high-sensitivity pressure sensor, the diameter of the microcones is optimized and the microstructure morphologies are shown in Fig. S14. The pressure sensitivity ($S$) can be defined by $S = \delta(\Delta R/R_0)/\delta P$, where $\Delta R$ is the change of resistance under load of $P$, and $R_0$ is the base resistance without load. Fig. 3a shows the relative-resistance changes of the pressure sensor with microconed diameters of 20 and 30 μm, respectively. The sensitivity of the pressure sensor with 20 μm microcones is calculated to be 18.4% $kPa^{-1}$, which is much higher than that of the sensor with 30 μm microcones (8.47% $kPa^{-1}$), due to the larger changes of the contact area under same external pressure. Fig. 3b shows stable and reproducible responses of the pressure sensor (20 μm microcones) at an operating current no less than 50 μA. Since the total resistance of the self-powered pressure sensing system is 234 Ω (r = 200 Ω,$R_0$ = 34 Ω), the minimal power generation of the TEG needs to reach 11.7 mV. By harvesting body heat, our flexible tf-TEG could generate an output voltage as large as 15.8 mV, thus the proposed tf-TEG could ensure stable operation of the sensor without an electronic boost (Fig. 2h).

### 2.4. Self-powered pressure sensing system

We developed a self-powered pressure sensing system by integrating the microconed pressure sensor with the flexible tf-TEG. As shown in Fig. 4a, the output voltage of the tf-TEG increases from 12.8 to 44.9 mV with the $\Delta T$ increasing from 3.3 to 11.5 K. Notably, the output voltage almost keeps constant when the applied pressure is increased from 0 to 12.4 kPa, implying that the TE voltage only relies on the $\Delta T$ across tf-TEG and is independent of the applied pressure. Fig. 4b shows that the load voltage of the sensor changes accordingly with the periodically applied external pressure at different $\Delta T$. The load voltage of the sensor gradually increases with the increasing $\Delta T$, attributed to the current of the whole circuit exceeding the working current of the sensor. To evaluate the sensitivity of the self-powered pressure sensor, the load-voltage changes of the sensor upon various pressure were measured when certain temperature gradients were applied to the tf-TEG (Fig. S15). The load voltages of the sensor decrease nearly exponentially with the increasing pressure (<12 kPa) due to the decrease of load resistance. Fig. 4c shows the relative voltage changes of the sensor versus the loading pressure. A linear relationship between the relative load-voltage change and pressure is observed at the low-pressure region (<5 kPa) and it is not affected by the temperature gradients. The sensitivity of the self-powered pressure sensor is 17.1%, which is comparable to that of the other reports (Inset of Fig. 4c) [38,39]. In addition, the sensitivity of the self-powered sensor is very close to that of the sensor driven by external power source (Fig. 3a). It is because that the relative load-voltage changes of the self-powered sensor approximately equals to the relative load-resistance change as illustrated in equation (4).

$$\frac{V_{L0}-V_L}{V_{L0}} = \frac{\frac{U_T}{R_0+r}\times R_0 - \frac{U_T}{R_L+r}\times R_L}{\frac{U_T}{R_0+r}\times R_0} = \frac{r}{R_L+r} \times \frac{R_0-R_L}{R_0} \qquad (r \gg R) \tag{4}$$

Where $U_T$ is the output voltage of the TEG at certain $\triangle T$, $R_0$ is the initial load resistance of the sensor.

According to equation (4), it is also clearly observed that the sensitivity of the self-powered sensing system is related to the load matching of the flexible th-TEG for pressure sensor. To further investigate the influence of the load matching of tf-TEG on pressure sensor, we also prepared tf-TEG with more *p-n* arrays and larger-sized TE legs on PI substrate (Fig. S16). As shown in Fig. S17, the open voltages from 36 *p-n* arrays are in a linear relationship with the temperature gradients (11.8–56.5 K), and the internal resistance of the 36 *p-n* arrays is 995 Ω. Based on the working principle of the self-powered pressure sensor, the ratio between internal resistance and load resistance (*r*:*R*) could be effectively adjusted by connecting different numbers of *p-n* arrays in

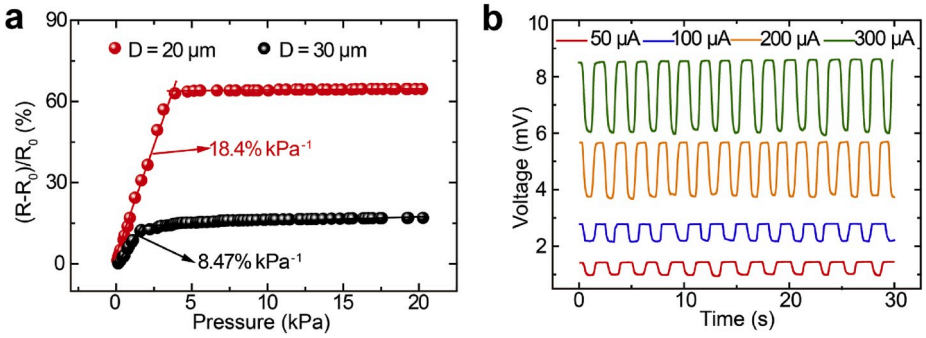


**Fig. 3.** Characterization of the microconed pressure sensor. (a) Relative-resistance changes of the pressure sensor with microconed diameters of 20 and 30 μm, respectively. (b) The voltage changes of the pressure sensor with 20 μm microcones at pressure of 310 Pa and a constant-current range from 50 to 300 μA.

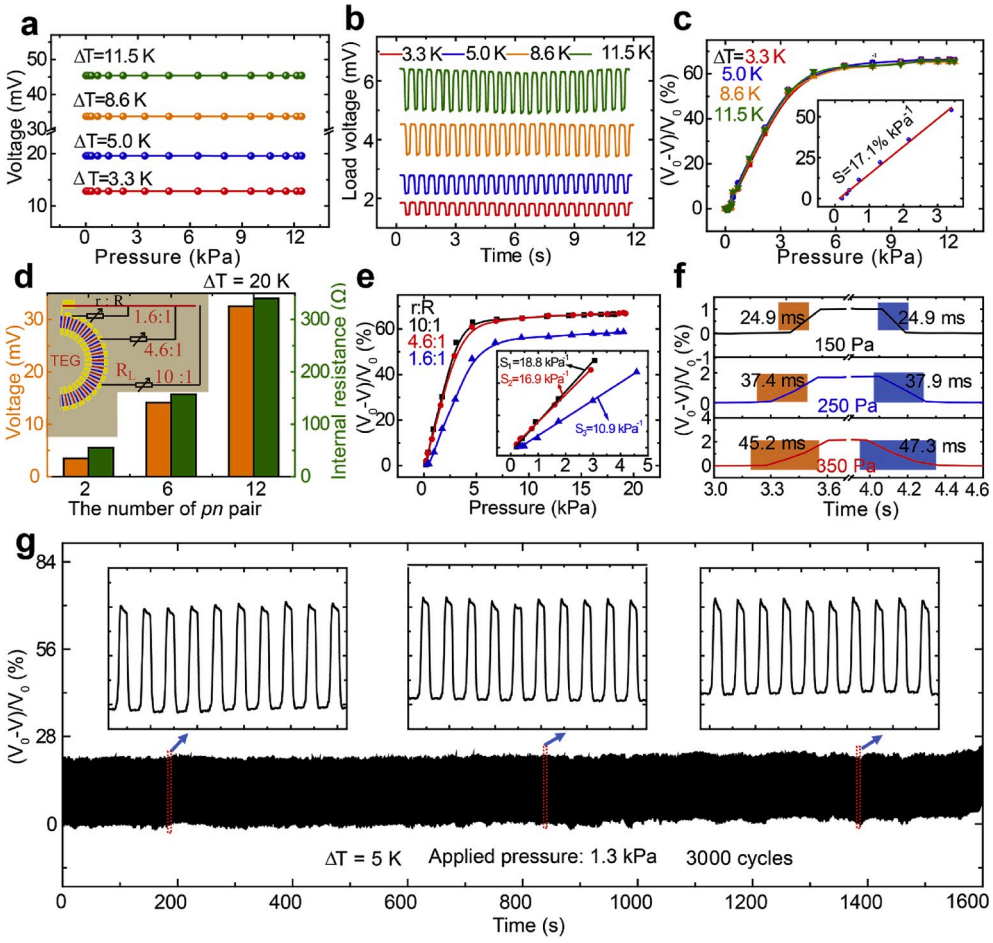


**Fig. 4.** Characteristic evaluation of the self-powered pressure sensing system. (a) Voltage variations of the tf-TEG against various pressures applied to the sensor under different temperature differences. (b) Load voltage of the pressure sensor under periodically applied pressure of 1.3 kPa at various ΔT across the tf-TEG. (c) Relative load-voltage variations of the sensing system versus applied pressure under various temperature gradients. (d) Output voltage and internal resistance of *pn* pairs obtained selectively from a 36 *pn* array ($\Delta T = 20$ K). (e) Relative load-voltage variations of the sensing system versus applied pressure under various ratios of *r:R*. (f) Response and relaxation time for the sensing system under cycling pressures of 150 Pa, 250 Pa, 350 Pa, respectively. (g) Stability of the sensor under 3000 loading/unloading cycles with applied pressure of 1.3 kPa.

series. Fig. 4d exhibits the various values of *r:R* were obtained by separately connecting the 2 *p-n* arrays, the 6 *p-n* arrays, and the 12 *p-n* arrays with the pressure sensor in series. It could be observed that the open voltage and internal resistance of the tf-TEG under 2 *p-n* arrays, 6 *p-n* arrays, and 12 *p-n* arrays at $\Delta T = 10$ K are consistent with the results in Fig. S17. The responses of the self-powered system to pressure were characterized at different ratios of *r:R* (Fig. S18). Obviously, they all exhibit stable signal output during the loading/unloading processes, and the relative load-voltage changes of the system with $r:R = 10$ is nearly equal to that with $r:R = 4.6$ but higher than that with $r:R = 1.6$. Fig. S19 shows load-voltage variations of the self-powered system under various ratios of *r:R*. The loading voltages decrease with the increasing pressure at a similar trend observed in Fig. S15. In addition, the sensitivity of the system is found to be highly dependent on the ratios of *r:R* (Fig. 4e). The self-powered pressure sensing system shows a higher sensitivity at a larger ratio of *r:R*. The reason is that when the ratio of r:R is larger (r≫R), the relative-voltage change of the pressure sensor is more close to the relative-resistance change of the sensor in the self-powered system according to Eq. (4). Namely, a larger ratio between the internal and load resistance is beneficial to improve the sensitivity of the self-powered sensing system.

For dynamic pressure-sensing, the response time and repeatability of the self-powered pressure sensing system are crucial. We characterized the dynamic response of the sensing system under cycling pressures of 150, 250, and 350 Pa (Fig. 4f and Fig. S20). The responding time of the sensor is less than 47.3 ms under 350 Pa, which is close to the response

time of real human skin from 30 to 50 ms [40]. Additionally, stability of the self-powered sensing system was investigated under $\Delta T = 5$ K across the tf-TEG (Fig. 4g). The load voltage of the sensor remains stable and periodic variation during 3000 loading/unloading cycles.

### 2.5. Wearable applications for human healthcare monitoring and motion detection

To assess the health monitoring capabilities of the self-powered pressure sensing system, the flexible tf-TEG was directly taped on human skin to harvest body heat while the flexible pressure sensor was attached to different parts of the human body to monitor physiological signals and motion activities. As demonstrated in Fig. 5a, the pressure-sensing system was attached at the wrist to monitor the pulse signals. The detailed experimental setup is displayed in Fig. 5b. Pulse signals measured from a volunteer's wrist is sampled, and then transmitted to a laptop for visualization and analysis. Fig. 5c shows the wrist pulse wave patterns for a 26-year-old male volunteer and a 28-year-old female volunteer measured with the self-powered pressure sensing system (Supporting Information Movies). The pulse shapes are all regular and repeatable, but pulse frequency of the male is slower than that of the female. Three characteristic peaks of wrist pulse, including percussion wave (P), late systolic pulse waveform (T) and diastolic pulse waveform (D) were clearly observed and distinguished, demonstrating a high detecting resolution of the self-powered sensing system (Fig. 5d) [41]. Besides, we also find that the P-wave and T-wave of a male are faster and stronger, implying a greater momentum of blood ejection compared with that of a female [5]. These results demonstrate great promises of our proposed pressure-sensing system for applications in physiological diagnosis. Furthermore, vigorous human motions could also be detected with the proposed system. Fig. 5e–g shows the capability of the system in real-time monitoring of various human motions including cheek-bulge, palm-bend, and wrist motion, which could find useful applications in clinical assessment of motor disorders, rehabilitation and robotic control.

## 3. Conclusion

In summary, we have demonstrated a self-powered wearable pressure sensing system consisting of a micropatterned pressure sensor and a flexible tf-TEG with specially designed absorber and heat sink for high power generation. The flexible tf-TEG enables continuously powering the pressure sensor without an electronic boost circuitry. On this basis, the self-powered pressure sensing system achieved a fast response time (24.9 ms), high sensitivity (17.1% $kPa^{-1}$) and excellent durability (over 3000 cycles with a pressure of 1.3 kPa). Moreover, the sensitivity of self-powered pressure sensing sensor system was independent of the temperature gradients across the tf-TEG but could be controlled by the ratio of the internal resistance and load resistance. It was further shown that the pressure sensing system can be used for real-time monitoring of diverse physiological signals and body motions by harvesting human body heat as power source. Our investigations are expected to promote the commercialization of self-powered wearable electronics using thin-film thermoelectric generators, especially for wearable healthcare devices.

## 4. Experimental section

*Preparation of the Flexible tf-TEG*: The tf-TEG with 25 pairs of thermoelectric legs was deposited on the polyimide (PI) substrate in magnetron sputtering system (JGP-450a, SKY Technology Development Co., Ltd, Chinese Academy of Sciences). Stainless steel masks, designed with various patterns and sizes, were employed for sputtering thin-film materials of the TEG. Initially, the $Bi_2Te_3$ was fixed on a direct current (DC) power with 20 W, while the Te target was placed on a radio frequency (RF) power with 20 W. The $Sb_2Te_3$ target was driven by a DC power supply of 20 W, and the Te target was connected to a RF power with 31 W. Then, the n-type and p-type films were sequentially fabricated at 350 °C for 4 h with Ar working pressure of 2 Pa. Finally, Cu thin-film electrodes were sputtered on the top of the TE films to connect the TE legs where the working pressure of Ar was kept at 1.6 Pa. All targets with 60-mm-diameter (99.99% purity) were brought from General Research Institute for Nonferrous Metals.

*Preparation of the Thermal-Conductivity Insulating Materials*: Liquid PDMS precursors (Dow Corning Sylgard 184) were prepared at a base to curing agent ratio of 10:1 and thoroughly stirred for at least 10 min. BN with average diameter of 15 or 30 μm (Dandong Rijin Science and Technology Co.) was mixed into the as-prepared PDMS, followed by

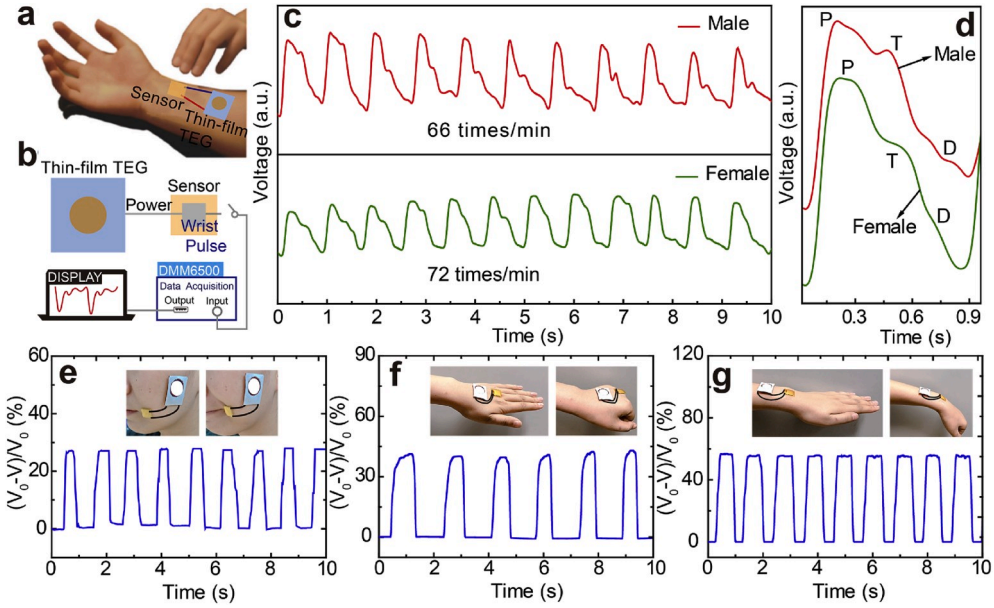


**Fig. 5.** Real-time monitoring of physiological signals and body motions. (a) A demonstration of wrist pulse monitoring with the self-powered pressure sensing system harvesting body heat. (b) Experimental setup for signal processing. (c) Wrist pulse signals of a 26-year-old male and a 28-year-old female volunteers, respectively. (d) Closeup of the pulse signals. (e–g) Response of the self-powered sensing system to (e) mouth shrug, (f) palm motion, (g) wrist motion.

sonication to obtain stable and homogenous suspensions with BN concentration varying from 0 to 30%. The suspensions were then spin-coated on precleaned glass slides and cured in vacuum oven for 30 min at 90 °C. After that, the PDMS/BN composite films (400 μm) were peeled off from the glass slides.

*Preparation of the hydrogel heat sink*: The flexible heat sink for TEG was prepared by employing the cooling gel patches which were acquired from Jinhua jingdi medical supplies company. The cooling gel patch consists of non-woven fabrics, hydrophilic polymeric hydrogels and plyethylene as displayed in Fig. S21. Among them, the hydrophilic polymeric hydrogels are three-dimensional network structure containing large water (80%). When the hydrogels were heated, it could effectively dissipate heat through water evaporation and cooling for 8 h in this work. Then, a cylinder was cut off in the cooling gel patches according to the cold-size of the TEG for achieving the hydrogel heat sink. After the plyethylene was moved, the cooing gel layer of heat sink was attached to the cold-side of the TEG.

*Finite element analysis (FEA)*: FEA was implemented by utilizing commercial package ANASYS/Workbench 19.2 to build TEG models. The electrical conductivity(σ), seebeck coefficient (S) and thermal conductivity of materials are set as Table S3. The convection coefficients and air temperature are 1 W $K^{-1}$ $m^{-2}$ and 25 °C. The open-circuit voltage is calculated by solving the heat transfer equation in a steady state.

*Preparation of the Self-Powered Pressure Sensing System*: Inverted microconed cavities on the Cu sheet (12 mm × 12 mm × 0.1 mm) were engraved as a mold by the laser engraving machine (VLS3.50, 50 W, Universal Laser System, USA) at power of 30% for 0.5 h (Fig. S12). The laser speed was fixed at 1 m/s. The liquid PDMS (Sylgard 184, Dow Corning) was then spin-coated onto each as-prepared Cu mold, and cured in vacuum oven for 30 min at 90 °C, after which the PDMS films were peeled off from the Cu master. Subsequently, a thin layer (Ti) was deposited on the microconed PDMS films for 15 min using magnetron sputtering technique, followed by sputtering Ag film on top of the Ti layer for 10 min. The sputtering power and Ar working pressure were fixed at 10 W and 2 Pa, respectively. The microstructured Ag/Ti/PDMS films were placed face-to-face on the PI film to prepare the pressure sensor. Finally, the self-powered wearable pressure sensing system was fabricated by connecting the pressure sensor with as-prepared tf-TEG in series.

*Characterizations and Measurements*: The morphology and structure of the thin films were observed by an optical microscope (Olympus MX61) and a field emission scanning electron microscope (FE-SEM). The X-ray diffraction (XRD, Rigaku D/MAX 2200 PC) was used to examine the crystal structure of the thin films. Seebeck coefficient (α) and conductivity (σ) of the TE films were measured by ZEM-3 (Ulvac Riko, Inc.). The measurements of thermal conductivity of the PDMS/BN films were conducted with a Thermal Interface Material Tester 1300 (Analysis Tech, Wakefield, MA USA). The bending test of the tf-TEG and the loading of applied force to the pressure sensor were separately carried out with an electric horizontal test machine (SJH-600, Shsiwi Co., Ltd.), while the electrical signals of the self-powered pressure sensing system were recorded at the same time by a digital source-meter (DMM6500).

## Declaration of competing interest

The authors declare that they have no known competing financial interests or personal relationships that could have appeared to influence the work reported in this paper.

## CRediT authorship contribution statement

**Yaling Wang:** Writing - review & editing, Conceptualization, Data curation, Methodology. **Wei Zhu:** Funding acquisition, Supervision, Writing - review & editing. **Yuan Deng:** Funding acquisition, Project administration, Resources. **Bo Fu:** Funding acquisition, Writing - review & editing. **Pengcheng Zhu:** Formal analysis, Software. **Yuedong Yu:** Visualization. **Jiao Li:** Investigation. **Jingjing Guo:** Writing - review & editing.

## Acknowledgements

The work was supported by the National Key R&D Program of China (Grant No. 2018YFA0702100 and 2018YFB2003200), the Joint Funds of the National Natural Science Foundation of China (Grant No. U1601213), the National Natural Science Foundation of China (Grant No. 51601005), the Beijing Natural Science Foundation (Grant No. 2182032), the Beijing Nova Programme Interdisciplinary Cooperation Project (Grant No. Z191100001119013), and the Fundamental Research Funds for the Central Universities.

## Appendix A. Supplementary data

Supplementary data to this article can be found online at https://doi.org/10.1016/j.nanoen.2020.104773.

## References

[1] W. Zeng, L. Shu, Q. Li, S. Chen, F. Wang, X. Tao, Fiber-based wearable electronics: a review of materials, fabrication, devices, and applications, Adv. Mater. 26 (2014) 5310–5336.
[2] A. Nag, S.C. Mukhopadhyay, J. Kosel, Wearable flexible sensors: a review, IEEE Sensor. J. 17 (2017) 3949–3960.
[3] T.Q. Trung, N.-E. Lee, Flexible and stretchable physical sensor integrated platforms for wearable human-activity monitoring and personal healthcare, Adv. Mater. 28 (2016) 4338–4372.
[4] Y. Chu, J. Zhong, H. Liu, Y. Ma, N. Liu, Y. Song, J. Liang, Z. Shao, Y. Sun, Y. Dong, X. Wang, L. Lin, Human pulse diagnosis for medical assessments using a wearable piezoelectret sensing system, Adv. Funct. Mater. 28 (2018) 1803413–1803422.
[5] X. Wang, Y. Gu, Z. Xiong, Z. Cui, T. Zhang, Silk-molded flexible, ultrasensitive, and highly stable electronic skin for monitoring human physiological signals, Adv. Mater. 26 (2014) 1336–1342.
[6] J. Guo, B. Zhou, C. Yang, Q. Dai, L. Kong, Stretchable and temperature-sensitive polymer optical fibers for wearable health monitoring, Adv. Funct. Mater. 29 (2019) 1902898–1902905.
[7] W. Yang, J. Chen, G. Zhu, J. Yang, P. Bai, Y. Su, Q. Jing, X. Cao, Z. Wang, Harvesting energy from the natural vibration of human walking, ACS Nano 7 (2013) 11317–11324.
[8] X. Meng, Q. Cheng, X. Jiang, Z. Fang, X. Chen, S. Li, C. Li, C. Sun, W. Wang, Z. Wang, Triboelectric nanogenerator as a highly sensitive self-powered sensor for driver behavior monitoring, Nano Energy 51 (2018) 721–727.
[9] B. Nie, R. Li, J. Cao, J.D. Brandt, T. Pan, Flexible transparent iontronic film for interfacial capacitive pressure sensing, Adv. Mater. 27 (2015) 6055–6062.
[10] J. Shi, L. Wang, Z. Dai, L. Zhao, M. Du, H. Li, Y. Fang, Multiscale hierarchical design of a flexible piezoresistive pressure sensor with high sensitivity and wide linearity range, Small 14 (2018) 1800819–1800825.
[11] Y. Zhang, Y. Hu, P. Zhu, F. Han, Y. Zhu, R. Sun, C.-P. Wong, Flexible and highly sensitive pressure sensor based on microdome-patterned PDMS forming with assistance of colloid self-assembly and replica technique for wearable electronics, ACS Appl. Mater. Interfaces 9 (2017) 35968–35976.
[12] B.J. Kim, D.H. Kim, Y.-Y. Lee, H.-W. Shin, G.S. Han, J.S. Hong, K. Mahmood, T. K. Ahn, Y.-C. Joo, K.S. Hong, N.-G. Park, S. Lee, H.S. Jung, Highly efficient and bending durable perovskite solar cells: toward a wearable power source, Energy Environ. Sci. 8 (2015) 916–921.
[13] J. Yoon, A.J. Baca, S.-I. Park, P. Elvikis, J.B. Geddes III, L. Li, R.H. Kim, J. Xiao, S. Wang, T.-H. Kim, M.J. Motala, B.Y. Ahn, E.B. Duoss, J.A. Lewis, R.G. Nuzzo, P. M. Ferreira, Y. Huang, A. Rockett, J.A. Rogers, Ultrathin silicon solar microcells for semitransparent, mechanically flexible and microconcentrator module designs, Nat. Mater. 7 (2008) 907–915.
[14] X. Cao, Y. Jie, N. Wang, Z. Wang, Triboelectric nanogenerators driven self-powered electrochemical processes for energy and environmental science, Adv. Energy Mater. 6 (2016) 1600665–1600685.
[15] Y. Jie, H. Zhu, X. Cao, Y. Zhang, N. Wang, L. Zhang, Z. Wang, One-Piece triboelectric nanosensor for self-triggered alarm system and latent fingerprint detection, ACS Nano 10 (2016) 10366–10372.
[16] Y. Jie, Q. Jiang, Y. Zhang, N. Wang, X. Cao, A structural bionic design: from electric organs to systematic triboelectric generators, Nano Energy 27 (2016) 554–560.
[17] S. Funahashi, T. Nakamura, K. Kageyama, H. Ieki, Monolithic oxide–metal composite thermoelectric generators for energy harvesting, J. Appl. Phys. 109 (2011) 124509–124513.
[18] Y. Yang, X. Wei, J. Liu, Suitability of a thermoelectric power generator for implantable medical electronic devices, J. Phys. D Appl. Phys. 40 (2007) 5790–5800.

[19] Y. Shi, Y. Wang, D. Mei, B. Feng, Z. Chen, Design and fabrication of wearable thermoelectric generator device for heat harvesting, IEEE Robot. Autom. Lett. 3 (2018) 373–378.
[20] C.S. Kim, G.S. Lee, H. Choi, Y.J. Kim, H.M. Yang, S.H. Lim, S.-G. Lee, B.J. Cho, Structural design of a flexible thermoelectric power generator for wearable applications, Appl. Energy 214 (2018) 131–138.
[21] C.S. Kim, H.M. Yang, J. Lee, G.S. Lee, H. Choi, Y.J. Kim, S.H. Lim, S.H. Cho, B. J. Cho, Self-powered wearable electrocardiography using a wearable thermoelectric power generator, ACS Energy Lett. 3 (2018) 501–507.
[22] S.J. Kim, J.H. We, B.J. Cho, A wearable thermoelectric generator fabricated on a glass fabric, Energy Environ. Sci. 7 (2014) 1959–1965.
[23] R. Tian, Y. Liu, K. Koumoto, J. Chen, Body heat powers future electronic skins, Joule 3 (2019) 1399–1403.
[24] D. Kong, W. Zhu, Z. Guo, Y. Deng, High-performance flexible Bi2Te3 films based wearable thermoelectric generator for energy harvesting, Energy 175 (2019) 292–299.
[25] W. Zhu, Y. Deng, L. Cao, Light-concentrated solar generator and sensor based on flexible thin-film thermoelectric device, Nano Energy 34 (2017) 463–471.
[26] P.J. Taroni, G. Santagiuliana, K. Wan, P. Calado, M. Qiu, H. Zhang, N.M. Pugno, M. Palma, N. Stingelin-Stutzman, M. Heeney, O. Fenwick, M. Baxendale, E. Bilotti, Toward stretchable self-Powered sensors based on the thermoelectric response of PEDOT:PSS/Polyurethane blends, Adv. Funct. Mater. 28 (2018) 1704285–1704292.
[27] D. Zhang, K. Zhang, Y. Wang, Y. Wang, Y. Yang, Thermoelectric effect induced electricity in stretchable graphene-polymer nanocomposites for ultrasensitive self-powered strain sensor system, Nano Energy 56 (2019) 25–32.
[28] B. Su, S. Gong, Z. Ma, L.W. Yap, W. Cheng, Mimosa-inspired design of a flexible pressure sensor with touch sensitivity, Small 11 (2015) 1886–1891.
[29] Y. Pang, K. Zhang, Z. Yang, S. Jiang, Z. Ju, Y. Li, X. Wang, D. Wang, M. Jian, Y. Zhang, R. Liang, H. Tian, Y. Yang, T. Ren, Epidermis microstructure inspired graphene pressure sensor with random distributed spinosum for high sensitivity and large linearity, ACS Nano 12 (2018) 2346–2354.
[30] T. Zhao, T. Li, L. Chen, L. Yuan, X. Li, J. Zhang, Highly sensitive flexible piezoresistive pressure sensor developed using biomimetically textured porous materials, ACS Appl. Mater. Interfaces 11 (2019) 29466–29473.
[31] Y. Gao, C. Lu, Y. Guohui, J. Sha, J. Tan, F. Xuan, Laser micro-structured pressure sensor with modulated sensitivity for electronic skins, Nanotechnology 30 (2019) 325502.
[32] M.-K. Kim, M.-S. Kim, S. Lee, C. Kim, Y.-J. Kim, Wearable thermoelectric generator for harvesting human body heat energy, Smart Mater. Struct. 23 (2014) 105002.
[33] F. Deng, H. Qiu, J. Chen, L. Wang, B. Wang, Wearable thermoelectric power generators combined with flexible supercapacitor for low-power human diagnosis devices, IEEE Trans. Ind. Electron. 64 (2017) 1477–1485.
[34] L. Zhao, B. Zhang, W. Liu, J. Li, Effect of mixed grain sizes on thermoelectric performance of Bi2Te3 compound, J. Appl. Phys. 105 (2009), 023704-023709.
[35] Q. Song, W. Zhu, Y. Deng, D. He, J. Feng, Enhanced thermal conductivity and mechanical property of flexible poly (vinylidene fluoride)/boron nitride/graphite nanoplatelets insulation films with high breakdown strength and reliability, Compos. Sci. Technol. 168 (2018) 381–387.
[36] S. Cui, Y. Hu, Z. Huang, C. Ma, L. Yu, X. Hu, Cooling performance of bio-mimic perspiration by temperature-sensitive hydrogel, Int. J. Therm. Sci. 79 (2014) 276–282.
[37] B. Zhu, Z. Niu, H. Wang, W.R. Leow, H. Wang, Y. Li, L. Zheng, J. Wei, F. Huo, X. Chen, Microstructured graphene arrays for highly sensitive flexible tactile sensors, Small 10 (2014) 3625–3631.
[38] L. Tao, K. Zhang, H. Tian, Y. Liu, D. Wang, Y. Chen, Y. Yang, T. Ren, Graphene-paper pressure sensor for detecting human motions, ACS Nano 11 (2017) 8790–8795.
[39] Y. Wei, S. Chen, Y. Lin, Z. Yang, L. Liu, Cu–Ag core–shell nanowires for electronic skin with a petal molded microstructure, J. Mater. Chem. C 3 (2015) 9594–9602.
[40] A. Chortos, Z. Bao, Skin-inspired electronic devices, Mater, Today 17 (2014) 321–331.
[41] P. Nie, R. Wang, X. Xu, Y. Cheng, X. Wang, L. Shi, J. Sun, High-performance piezoresistive electronic skin with bionic hierarchical microstructure and microcracks, ACS Appl. Mater. Interfaces 9 (2017) 14911–14919.

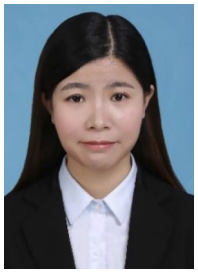

**Yaling Wang** is currently a Ph.D. student in Prof. Yuan Deng's group at Beihang University. She received her BS (2014) degree in Materials Chemistry at Henan Polytechnic University, and MS (2016) degree in Pharmaceutical Engineering at Beijing Institute of Technology. Her research interests include fabrication of thin film thermoelectric materials and fabrication of multi-functional sensing devices for human physiological monitoring.

**Wei Zhu** received her BS (2010) and PhD (2016) degrees of materials science and engineering from Beihang University (China). Then she stayed and worked at Prof. Yuan Deng's group in Beihang University. Now she is working as an Associate Research Fellow with research interests including the design, numerical simulation, fabrication of thin-film thermoelectric device and thermal metamaterials for thermal energy utilization and energy sensing.

**Yuan Deng** received his BS (1995) and PhD (2000) degrees in chemistry from Tsinghua University (China). After that, he worked as postdoctoral fellow of materials at Tsinghua University. Then he worked as associate professor at Beihang University. Since 2008, he served as professor in School of Materials Science and Engineering. He has mentored about 20 PhD students or postdoctoral researchers. He has authored and co-authored more than 130 papers. His main research interests are the design and fabrication of advanced energy materials and device, in particular low-dimensional thermoelectric material and device for energy management and conversion.

**Bo Fu** received his PhD degree from Tsinghua University in 2015. After two-years research in University of Cambridge, he began his independent career as an Associate Research Professor in Beihang University. He has authored and co-authored more than 40 peer-reviewed papers. His research interests include pulsed fiber lasers, ultrafast photonics, and 2D materials based nonlinear optics, etc.

**Pengcheng Zhu** is currently a Ph.D. student in Prof. Yuan Deng's group at Beihang University. He received his BS (2013) degree in macromolecular materials and engineering at Hubei University, and MS (2016) degree in materials science and engineering at Beijing University of Chemical Technology. His research interests include fabrication of organic piezoelectric materials and design and fabrication of multi-functional sensing devices for human physiological monitoring.

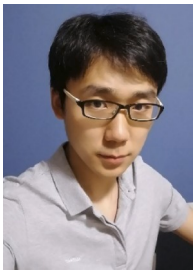

**Yuedong Yu** is currently a Ph.D. student in Prof. Yuan Deng's group at Beihang University. He received his BS (2012) degree in inorganic nonmetallic materials at University of Science & Technology Beijing, and MS (2014) degree in materials science and engineering at University of Sheffield. His research interests include fabrication of thin film thermoelectric materials and design and fabrication of thin film thermoelectric devices for cooling.

**Jiao Li** is currently a master student in Prof. Yuan Deng's group at Beihang University. She received her BS (2018) degree in Metal Materials and Engineering at Hebei University of Technology. Her research interests include fabrication of thin film thermoelectric materials and exploring the service performance of thermoelectric thin film materials.

**Jingjing Guo** received the B.S. degree in Optical information and science from Wuhan University of Technology in 2013. In 2018, he was granted the Ph.D. degree in Optical Engineering by Tsinghua University. Currently, he is a postdoctoral fellow at Tsinghua University. His research interests include fiber-optic sensors, wearable optics, and fiber lasers.

# Self-powered wearable pressure sensing system for continuous healthcare monitoring enabled by flexible thin-film thermoelectric generator

Wang, Yaling; Zhu, Wei; Deng, Yuan; Fu, Bo; Zhu, Pengcheng; Yu, Yuedong; Li, Jiao; Guo, Jingjing

01 ziwei Li Page 1

16/6/2021 0:26

□□□□□□□